CHEMICAL ENGINEERING TRANSACTIONS
VOL. 46, 2015
A publication of AIDIC
The Italian Association of Chemical Engineering
Online at www.aidic.it/cet
Guest Editors: Peiyu Ren, Yancang Li, Huiping Song

**ISBN** 978-88-95608-37-2; **ISSN** 2283-9216
DOI: 10.3303/CET1546003

# A New Interpretation Model for Transit Time Based on Impulse Oxygen Activation Logging Data

Yong Dong*[a, b, d], Chuansheng Wu[b], Haimin Guo[c], Qinghe Lv[d], Hongkui Li[d]

[a] School of Information and Mathematics of Yangtze University, Hubei, Jingzhou, 434023, China
[b] Mechanical Postdoctoral Station, Wuhan University of Technology, Wuhan, Hubei, 430070, China
[c] Key Laboratory of Exploration Technologies for Oil and Gas Resources, Ministry of Education, Yangtze University, Hubei, Wuhan, 430100, China
[d] Institute of Petroleum Engineering Technology, Zhongyuan Bureau of Petroleum Exploration, Puyang, Henan, 457001, China

dongyong80@126.com

Aiming at the interpretation problem for impulse oxygen activation logging data, the number of the peak shape functions which are used to fit the interpretation model is very large and the logging interpretation accuracy of the function is low. And the accuracy of the weighted average interpretation model is also low. This paper presented an indirect method of selecting spectral peak. And it gave a new transit-time interpretation model. The specific operations are described as follow. Firstly, the background spectrum was chosen manually. And then several spectral peaks were determined according to the given rules. Finally, the determined spectral peak sections were substitute into the established transit-time interpretation model, and then the volume flow rate was calculated. The processing results of the measured data showed that the effect of the selecting methods of background spectrum on the interpretation results of interpretation model is very small and the interpretation accuracy is higher than the one of the existing model.

## 1. Introduction

The impulse oxygen activation logging technique directly monitors the transport of the activated oxygen atoms without being affected by the factors, such as the fluid salinity, viscosity, formation porosity, and so on. This technique can also monitor the Oxygen fluid transport of the annulus space through tubing. The technique is widely used in some large oilfield in china [XIE Ronghua, 2007; WU Qi et al, 2011; LI Chunzhou, 2009; Ma Yuwu, 2012; Wang Lingen, et al, 2010; GUO Haimin, et al, 2007].

The function fitting interpretation model [LIU Guoliang, 2006; DONG Wu, 2013; DONG Wu, et al, 2013; MA Huanying, 2013] thinks that the time spectrum corresponds to some kind of function, such as exponential function, Gaussian function et al. And this function has some unknown parameters. The interpretation process is described as follow: The first step is to select the function form, and then using the function fitting method determines the unknown parameters. Thus the transit-time is obtained. At last, the volume flow rate can be calculated. There are some deficiencies about this method. The number of peak shape functions is very lager. The problem of automatic selection of the peak shape function has not been solved yet. It also lacks the standard selection method which is used to calculate the spectral peak section by fitting.

The accuracy of the conventional weighted average interpretation model [LIU Guoliang, 2006; Wang Laixue, 2013] is poor. The reason is that the differences of recognition level of the interpretation workers lead to different methods of selecting spectral peak which lead to different interpretation flow rates, sometimes the differences are too large.

This paper presents an indirect way of selecting spectral peak, and gives a new transit-time interpretation model. The interpretation accuracy of new model is satisfying.

Please cite this article as: Dong Y., Wu C.S., Guo H.M., Lv Q.H., Li H.K., 2015, A new interpretation model for transit time based on impulse oxygen activation logging data, Chemical Engineering Transactions, 46, 13-18 DOI:10.3303/CET1546003

## 2. The indirect method of selecting spectral peak

### 2.1 The preprocessing of time spectrum

The measured time spectrum is showed in Fig. 1.

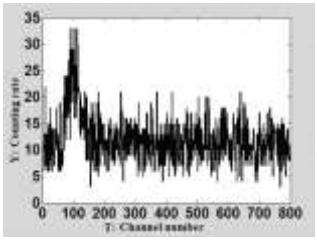


*Figure 1: The measured time spectrum*

The time spectrum showed in Fig. 1 comes from the measured data in one oilfield. It gives the data which is recorded by probe D2 of the impulse oxygen activation instrument. The abscissa of the figure represents the channel number and the ordinate represents the counting rate. That is, if we view time spectrum as array, channel numbers equal to sequence numbers of the element in array, the maximum figure of channel number means the number of elements in time spectrum array. There exists strong statistical fluctuation phenomenon and noise signal about this time spectrum, so it is not good for subsequent processing operation. Traditionally, we adopt multipoint moving average method to filtering. This paper introduces the method of the hard threshold filtering which is based on wavelet transform to smoothing the measured time spectrum. Fig. 2 shows the result of smoothing to the time spectrum.

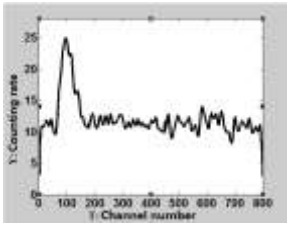


*Figure 2: The time spectrum after smoothing*

### 2.2 The selection of the background section

In Fig. 3, the spectral peak is identify artificially, and we choose the approximate horizontal segment which is near to the spectral peak. The approximate horizontal segment is that the counting rate fluctuates up and down in a horizontal line and the amplitudes are almost the same and that the whole variant trend is approximately horizontal.

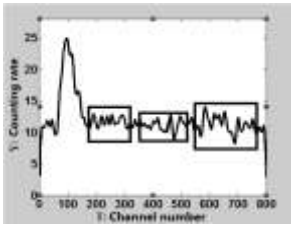


*Figure 3: The sketch map of the selection of the background section*

Each box in Fig. 3 corresponds to a certain way for background section selection. We can also get that there are several selections for background section.

### 2.3 The selection of spectral peak sections A, B, C, D, E

For the $CO_2$ flow time spectrum after smoothing, we determine the mean valve $\mu$ and mean square deviation $\sigma$. We determine the spectral peak section A according to the criterion $y > \mu + 2\sigma$. Denote the difference $f_A$ between the maximum counting rate $y_{A\max}$ and minimum counting rate $y_{A\min}$.

The difference, $f_A$, of the spectral peak section A is divided equally, and determine the spectral peak sections B, C, D and E. The concrete procedures are described as follow.

**Step 1** Let $y_B = y_{A\min} + 0.2 f_A$. Starting with the initial position of the spectral peak section A, search the time spectra point whose counting rate is most close to $y_B$ towards the right. Take the time spectra point as the initial point of the spectral peak section B.

**Step 2** Starting with the terminal position of the spectral peak section A, we search the time spectra point whose counting rate is most close to $y_B$ towards the left. We take the time spectra point as the terminal point of the spectral peak section B.

**Step 3** According to the initial point and terminal point of the spectral peak section B, we can determine the spectral peak section B.

**Step 4** Note $y_C = y_{A\min} + 0.4 f_A$, $y_D = y_{A\min} + 0.6 f_A$ and $y_E = y_{A\min} + 0.8 f_A$. According to the above method, determine the spectral peak section C, D and E, respectively.

## 3. The new transit-time interpretation model

Because the weighted average model is sensitive to the selection of the initial and terminal number of channel of the spectral peak, the small change of the initial and terminal channel number of the spectral peak will result in great change of interpretation flow. Therefore we built the following transit-time $t_m$ interpretation model.

$$t_m = \frac{1}{5} \times \left( \frac{\sum_{i=T_{A,1}}^{T_{A,2}} y_i t_i}{\sum_{i=T_{A,1}}^{T_{A,2}} y_i} + \frac{\sum_{i=T_{B,1}}^{T_{B,2}} y_i t_i}{\sum_{i=T_{B,1}}^{T_{B,2}} y_i} + \frac{\sum_{i=T_{C,1}}^{T_{C,2}} y_i t_i}{\sum_{i=T_{C,1}}^{T_{C,2}} y_i} + \frac{\sum_{i=T_{D,1}}^{T_{D,2}} y_i t_i}{\sum_{i=T_{D,1}}^{T_{D,2}} y_i} + \frac{\sum_{i=T_{E,1}}^{T_{E,2}} y_i t_i}{\sum_{i=T_{E,1}}^{T_{E,2}} y_i} \right) - \frac{1}{2} t_h \tag{1}$$

where, $t_h$ represents the duration of neutron burst. $T_{A,1}$ and $T_{A,2}$ represent the channel number corresponding to the initial point and terminal point of the spectral peak section A, respectively.

$T_{B,1}$, $T_{B,2}$, $T_{C,1}$, $T_{C,2}$, $T_{D,1}$, $T_{D,2}$, $T_{E,1}$ and $T_{E,2}$ respectively represent the channel number corresponding to the initial and terminal point of the spectral peak section B, C, D and E. $y_i$ represents the counting tare of the *i*th channel. $t_i$ represents the time of the *i*th channel.

## 4. The application example

This paper verifies the interpretation accuracy of the new interpretation model from two aspects. Firstly, according to the measured spectrum showed in Fig. 1, we compare the treatment effect of the weighted average model and the presented model, in Fig. 4, the result come from the function fitting model is shown in Fig. 5. And then, for the measured data of the different depth of different well, we analyze the interpretation effect of the presented interpretation model, in Fig. 6.

The volumetric flow model is showed as follow.

$$Q_V = PC \times \frac{L}{t_m}. \tag{2}$$

In the Eq. (2), $t_m$ represents the transit-time. $PC$ represents the pipe constant. $L$ represents the source spacing.

### 4.1 The comparison of the weighted average interpretation model and the presented model

For the time spectrum after smoothing showed in Fig. 2, we deal with it by using the weighted average interpretation model. The different ways of selecting peak and the corresponding interpretation flow rate are showed in Fig. 4.

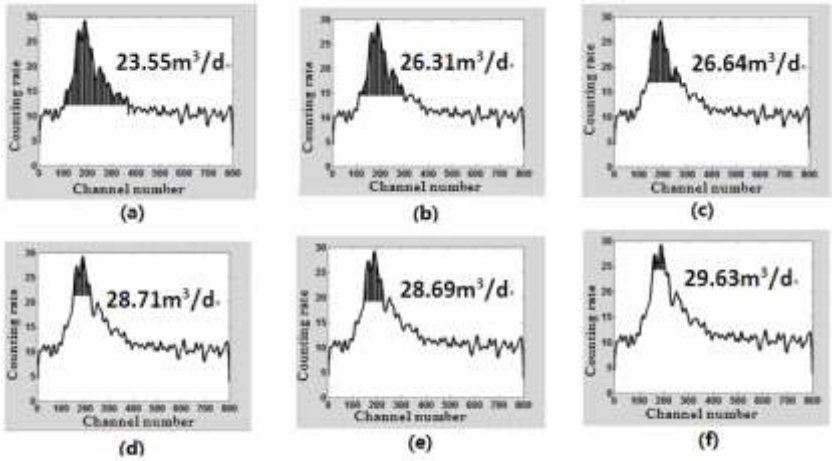


*Figure 4: The interpretation flow rate of the weighted average model under different ways of selecting peak*

In Fig. 4 the shaded area represents the initial and terminal channel number for the selecting peak artificially, and it shows the different ways of selecting peak intuitively. In Fig. 4, the flux data from (a) to (f) are the volume flow rates which are calculated by the weighted average interpretation model. It can be seen that the absolute deviation of the interpretation flow rate corresponding to different ways of selecting peak can reach 6.04 $m^3/d$ and the relative deviation based on the maximum interpretation flow rate can reach 20.4%. Obviously, it is difficult to control the interpretation accuracy to use the weighted average interpretation model.
MA Huanying, et al (2013) have given the specific function form for function fitting model. For the time spectrum showed in Fig. 2, the result from the function fitting model is shown as Fig. 5.

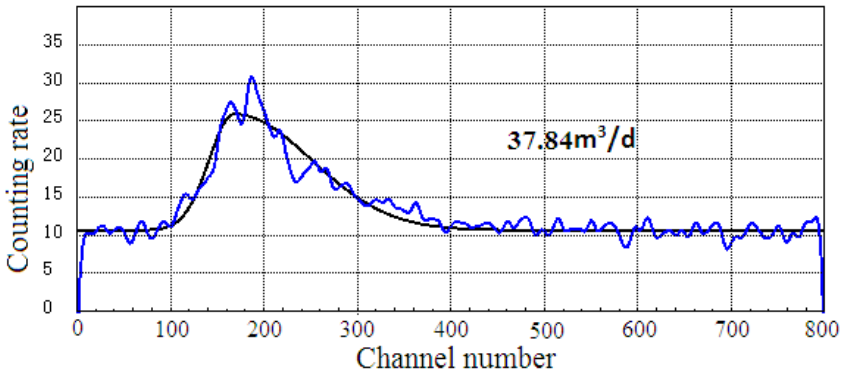


*Figure 5: Interpretation flow rate of function fitting model*

The interpretation flow rate is 37.84$m^3/d$, it is larger than the flow rates come from the other interpretation models. The difference indict that the accuracy of function fitting model is lower than the other two interpretation models.
For the time spectrum showed in Fig. 2, based on the method of selecting peak which is presented in this paper and the transit-time interpretation model, and combining the interpretation model of volume flow rate, Fig. 6 shows the different selecting ways of the background section and the corresponding interpretation flow rate.
Fig. 6 shows that the interpretation model which is presented in this paper is insensitive to the selecting ways of background section. In Fig. 6, the boxes present the selection ways of background sections, the short line segments nearly horizontal reflect the peak section A, B, C, D and E.

For the time spectrum showed in Fig. 2, the flow differences caused by different selecting ways of background section are little than 0.01 $m^3/d$.

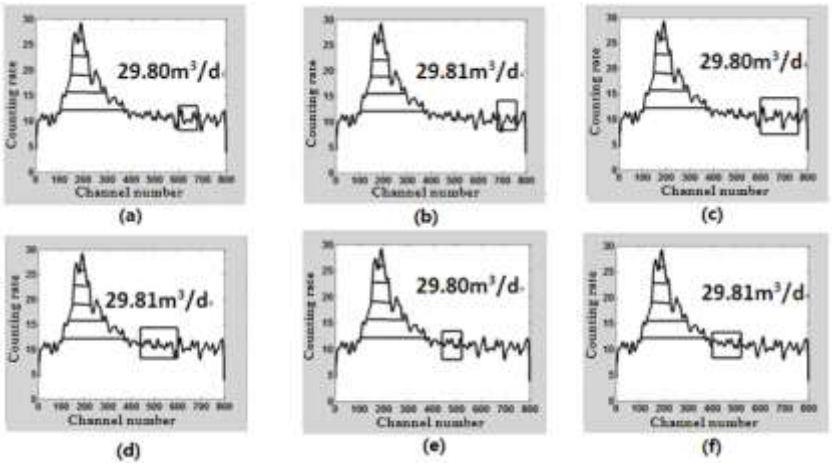


*Figure 6: The different ways of background section and the corresponding interpretation flow rate*

**4.2 The verification based on the repetitive measured data**

In order to verify the effect of the interpretation model presented in this paper, we measure the time spectrum repeatedly for the same measuring point. The time interval between the repetitive measures is only is between 1 and 2 minutes. So it can be considered theoretically that the time spectrum of repeated measure should have consistency. This means that the flow volumetric flow rates corresponding to the time spectrum of repeated measure should approximately equal. The data showed in Table 1 comes from some oilfield. The measuring point information and interpretation flow rate are showed in Table 1.

*Table 1: The treatment effect of the interpretation model in this paper*

| Well No. | X1 | | X2 | | X3 | | X4 | | |
|---|---|---|---|---|---|---|---|---|---|
| Measuring depth(m) | 175.5 | | 810.1 | | 2266.0 | | 2310.1 | | |
| Pressure (MPa) | 9.01 | 9.0 | 8.33 | 8.33 | 20.2 | 20.2 | 20.2 | 21.9 | 21.9 |
| Temperature (C) | -1.46 | -1.49 | 33.4 | 33.4 | 67 | 67 | 67 | 68.6 | 68.6 |
| Volume flow rate （$m^3/d$） | 171.4 | 170.4 | 29.5 | 29.7 | 139.3 | 140.4 | 142.6 | 78.2 | 79.1 |
| Relative deviation | 0.6% | | 0.7% | | 2.0% | | 1.1% | | |

From Table 1, we can see that the relative deviation of the interpretation flow rate of the interpretation model presented in this paper is less than or equal to 2% for the repetitive measuring data of the fixed measuring point. The result reflects the preferable interpretation accuracy. But when we use the weighted average model to deal with the data, we must carefully select the appropriate spectral peak to get good consistency for the interpretation flow rate.

## 5. Conclusions

(1) The way of selecting spectrum peak has negative effects on the conventional weighted average interpretation model and function fitting interpretation model. The method of the selecting background section has a strong operability. And the effects of the different selecting ways on the final interpretation results are negligible.

(2) The model presented in this paper select spectral peak automatically base on the background section. The interpretation accuracy is improved without increasing the manual labor intensity.

(3) The further studies on the time spectrum maybe can learn from the ideas provied b by ZHONG Qiubo, 2015, LING Tang, 2015, WANG Lei, 2014; TU Jihui, 2014.

**Acknowledgements**

The authors will thank people in Institute of Petroleum Engineering Technology, Zhongyuan Bureau of Petroleum Exploration for their great help. This paper is supported by National Natural Science Foundation of China (61273179, 61170031 and 60873021) and Natural Foundation of Hubei Province of China (2013CFA053). It is also supported by Educational Commission of Hubei Province of China (Q20121216) and scientific research projects of Hubei Province of China (B2015449).

**References**

Dong W., 2013, The Analysis and Study on Separation of Overlapping Peaks in the Time Spectrum of Oxygen Activation Logging, Applied Mechanics & Materials, 318: 601-606. DOI: 10.4028/www.scientific.net/AMM.318.601

Dong W., Guo H.M., Qi X,, 2013, The Disposal of Tailed Peak in the Time Spectrum of Pulsed Neutron Oxygen Activation Logging, Applied Mechanics & Materials, 318: 567-571. DOI: 10.4028/www.scientific.net/AMM.318.567

Guo H.M., Du W.J., Dai J.C., et al. 2007, Interpretation Method for Oxygen Activation Logging, JOURNAL OF OIL AND GAS TECHNOLOGY, 29(4): 94-96. DOI: 10.3969/j.issn.1000-9752.2007.04.018

Li C.Z., Qian J., Du S.S., et al. 2009, Application of pulsed-neutron oxygen activation water flowage logging tool (WFL) in Jiangsu oilfield, Petroleum Instruments, 23(01): 37-40. DOI: doi: 10.3969/j.issn.1004-9134.2009.01.012

Ling T., 2015, Super-resolution Reconstruction Method Integrated With Image Registration. REVIEW OF COMPUTER ENGINEER STUDIES, 2(1): 29-32.

Liu G.L., Liu X.W., Progress, 2006, Calculation Method of Water Flow Velocity in Impulse Oxygen Activation Log. WELL LOGGING TECHNOLOGY, 30(6): 548-550. DOI: 10.3969/j.issn.1004-1338.2006.06.016

Ma H.Y., Zhao J., Wu L.J., et al. 2013, On Water Flow Time Spectrum Interpretation Method in Oxygen Activation Log, WELL LOGGING TECHNOLOGY, 37(4):368-373. DOI: 10.3969/j.issn.1004-1338.2013.04.006

Ma Y.W., Chen M.Q., 2012, Application of Pulsed Neutron Oxygen Activation Water Logging in Western Oil Recovery Factory, Guangzhou Chemical Industry, 40(08): 163-165. DOI: 10.3969/j.issn.1001-9677.2012.08.060

Tu J.H., 2014, A Novel Building Boundary Extraction Method for High-resolution Aerial Image. REVIEW OF COMPUTER ENGINEER STUDIES, 1(2): 19-22.

Wang L.X., 2013, Effect evaluation between spectral flowing logging and multifunction flowing logging based on impulse oxygen activation logging technology, Petroleum Instruments, 27(05): 41-43. DOI: 10.3969/j.issn.1004-9134.2013.05.014

Wang L., 2014, An Ungreedy Chinese Deterministic Dependency Parser Considering Long-distance Dependency, REVIEW OF COMPUTER ENGINEER STUDIES, 1(2): 1-4.

Wang L.G., Wu L.J., Huang Z., Du Y.A., 2010, Application of oxygen activation water flow logging in bohai oilfield. Well Logging Technology, 34(1): 64-68. DOI: 10.3969/j.issn.1004-1338.2010.01.014

Wu Q., Li G.X., Liu J.P., et al. 2011, Progress, Needs & Prospected of Cased-hole Logging Technologies in Petro China. WELL LOGGING TECHNOLOGY, 35(6): 497-501. DOI: 10.3969/j.issn.1004-1338.2011.06.001

Xie R.H., 2007, Recent Progress and Orientation of Oilfield Dynamic Monitoring Technologies in China. WELL LOGGING TECHNOLOGY, 31(2): 103-106. DOI: 10.3969/j.issn.1004-1338.2007.02.003

Zhong Q.B., Zhao J., Tong C.Y., 2015, Motion Planning of Humanoid Robot Based on Embedded Vision. REVIEW OF COMPUTER ENGINEER STUDIES, 2(1): 33-36.